NASA TECHNICAL NOTE

NASA TN D-2025

NASA TN D-2025

THE NONLINEAR RESPONSE OF WINDOWS TO RANDOM NOISE

by Henry S. Freynik, Jr.

Langley Research Center
Langley Station, Hampton, Va.

NATIONAL AERONAUTICS AND SPACE ADMINISTRATION • WASHINGTON, D. C. • DECEMBER 1963

TECHNICAL NOTE D-2025

THE NONLINEAR RESPONSE OF WINDOWS TO RANDOM NOISE

By Henry S. Freynik, Jr.

Langley Research Center
Langley Station, Hampton, Va.

NATIONAL AERONAUTICS AND SPACE ADMINISTRATION

NATIONAL AERONAUTICS AND SPACE ADMINISTRATION

TECHNICAL NOTE D-2025

THE NONLINEAR RESPONSE OF WINDOWS TO RANDOM NOISE*

By Henry S. Freynik, Jr.

SUMMARY

The stress response of a 36-inch-square, 1/8-inch-thick window-glass plate mounted in putty on wooden frames was measured into the nonlinear range for both uniform static pressure and for random noise. It was determined from the stresses and frequencies that this edge mounting approximated simply supported conditions. The measured center stresses were in agreement with the nonlinear theory for static loading. The location of the maximum tensile stress in the plate was observed to migrate away from the center of the plate along the diagonals; this result was not anticipated by the available theoretical analyses.

The peak tensile stresses at the center of the plate exposed to random noise were compared with theoretical stresses estimated by the procedure of Miles. Good agreement was observed at low noise levels where the plate response was approximately linear. At higher noise levels the response became increasingly nonlinear in a hard-spring manner, and hence the theory overestimated the actual stresses.

INTRODUCTION

A general research program is currently in progress at the NASA Langley Research Center to study the noise-induced damage to ground building structural components. This problem will be important in the operation of future large ground-launched space exploration vehicles for which intense noise fields will extend over large areas around the launch site, and for which this radiated noise energy will peak in the frequency range corresponding to the natural vibration modes of ground building structures. Basic building response data are thus required for use in establishing criteria for the location of launch sites to minimize possible damage in surrounding communities. A possibility of window breakage due to this radiated booster noise has led to an investigation of stresses in a residential-type window exposed to high-intensity random noise. This report presents the measured results of this investigation and makes some comparisons with theory.

---

*Some of the information in this report was previously included in an article by the author entitled "Response of Windows to Random Noise," published in Sound, vol. 2, no. 3, May-June 1963, pp. 31-33.

SYMBOLS

a	span of square plate
A	plate surface area, a^2
E	modulus of elasticity
f	natural frequencies
k	stiffness
m,n	integers
q	uniform pressure
q_o	atmospheric pressure (14.7 lb/sq in.)
t	plate thickness
V	volume
V_o	enclosure volume
γ	ratio of specific heats (1.4 for air)
δ	damping as fraction of critical damping
ϵ	strain
μ	Poisson's ratio
σ	stress

TEST SPECIMENS AND PRELIMINARY STUDIES

Test Models

The type of window used in this study is illustrated schematically in figure 1. The window was a 36-inch-square plain window having double strength glass 1/8 inch thick. The glass was mounted on its frame with glazier's points and sealed with putty as in conventional residential construction. This mounting is illustrated in the right-hand sketch of the figure. The putty was allowed to age and cure for 6 to 8 months before testing so that the putty could attain its maximum working strength and provide a more typical edge condition.

For all practical purposes glass is an isotropic, homogeneous material and can be analyzed by standard plate theory. Glass has a linear stress-strain curve

with a modulus of elasticity E approximately equal to 10×10^6 pounds per square inch and a Poisson's ratio of 0.23, on the average (ref. 1). The weight density of this glass was approximately 0.0894 lb/cu in. Experience of other investigators in this field has shown that glass failure always results from a tensile component of stress (refs. 1 and 2).

For dynamic tests the window was mounted on an enclosure, as shown in the bottom sketch of figure 1, with a volume V_o of 15 cubic feet.

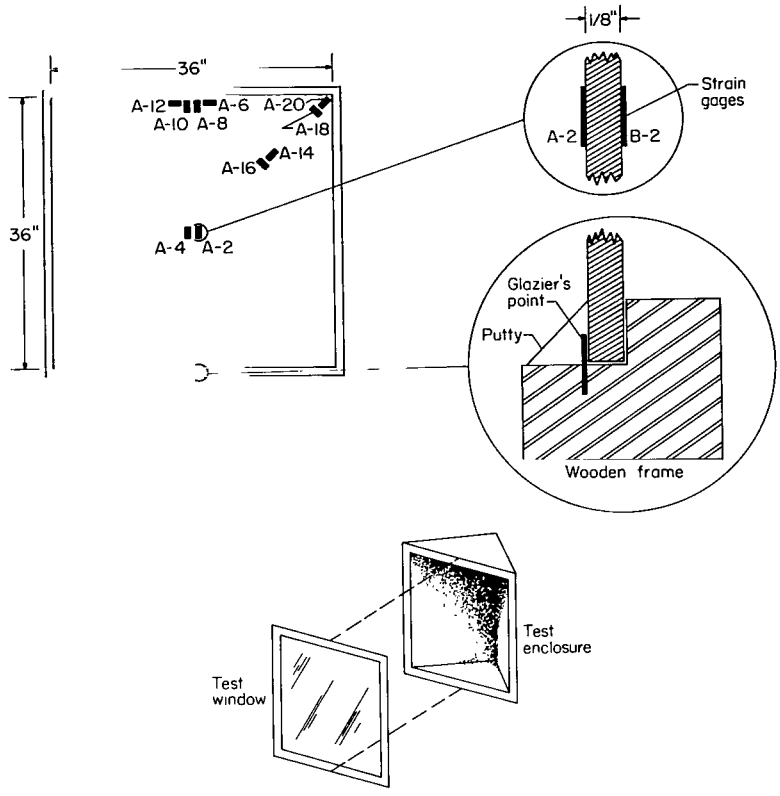

Figure 1.- Test models, enclosure, and strain-gage locations.

Stress Analysis

It was anticipated from the literature (for example, ref. 3) that the windows would respond in a nonlinear manner at all but the very lowest sound-pressure levels. Bending stresses predominate at low noise input levels where the plate center deflection is less than the plate thickness. At the higher noise levels, and hence at the larger center deflections, the applied load will be reacted upon in part by direct (or membrane) stresses in the middle surface of the plate. As the load increases, this membrane stress will become an increasingly greater percentage of the total outer fiber stress.

Experimental measurement of the static stress distribution in the window was necessary for three reasons. First, it was desirable to determine the degree of edge fixity. Second, all available theories, as summarized in reference 3, assume the maximum simply supported plate stress to occur at the center of the plate. However, experience of various experimenters (refs. 4 and 5) has shown that the location of this maximum outer fiber stress lies along a diagonal of the plate and in a direction perpendicular to it. This location appears to be a function of both the applied load and the ratio of plate thickness to span (ref. 5). Further information was desired in this respect so that the minimum number of dynamic gages would be required. Finally, in order to apply the dynamic stress response theory, it was necessary to measure the stress response of the system per unit static pressure.

For the purpose of reviewing the nature of this combined stress field in the plate, the schematic diagrams of figure 2 are presented. If an element of the plate is subjected to a pure bending moment as indicated in figure 2(a), the familiar antisymmetrical bending stress pattern exists. This pattern varies linearly from tension on one side of the plate to compression on the other side and is zero at the neutral axis of the plate. This stress is the only significant stress present in the plate when the center deflections are less than the plate thickness. At higher plate deflections direct stresses appear, and their distribution across the plate thickness is shown in figure 2(b). This direct stress or membrane stress is uniform across the plate thickness. In the general case, then, both bending and membrane stresses exist at any point in the plate. It can be seen that a gage at location X in figure 2(c) measures the sum of the membrane and bending stresses, whereas a strain gage at location Y measures the difference between the membrane and bending stresses.

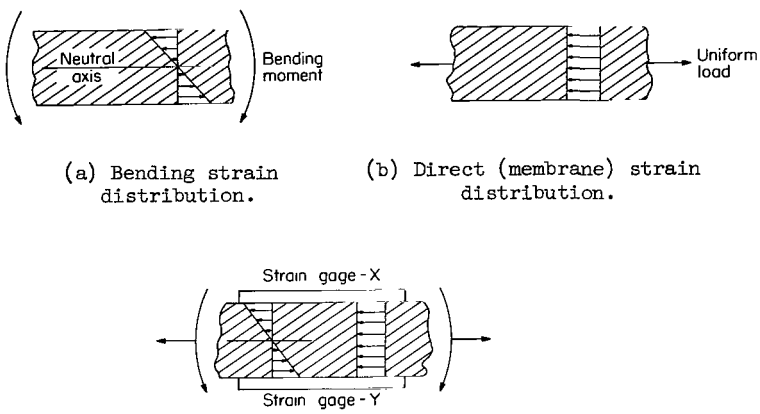

(a) Bending strain distribution.

(b) Direct (membrane) strain distribution.

(c) Combined loading.

Figure 2.- Strain distributions across window thickness.

For the gage locations considered the principal stress directions were assumed to lie along the lines of symmetry and perpendicular to them. With the principal stress directions so assumed, the principal stresses can be evaluated by measuring the corresponding principal strains in the directions of the principal stress axes. The principal stresses can be calculated from these principal strains by the following biaxial stress equation from reference 6:

$$\sigma_1 = \frac{E}{1 - \mu^2}\left(\epsilon_1 + \mu\epsilon_2\right)$$

where the subscripts 1 and 2 refer to the principal stress directions. At the center of the plate the strain in only one direction need be measured, because the stress field, from symmetry, is assumed the same in all directions.

Static Instrumentation and Test Procedures

For the static test, the windows were bolted securely to a plywood panel with a layer of putty between the plywood and the window frame to prevent air leakage. The putty side of the window was mounted facing the plywood, and air pressure was introduced into the intermediate space so that the differential

pressure exerted a force on the putty side (high-pressure side) of the glass. Hence, the wooden window frame instead of the glazier's points and putty reacted to the pressure load. The differential pressure applied to the window was monitored on a water manometer board.

Bonded resistance strain gages were mounted back-to-back on both sides of the plate in sufficient array (fig. 1) to permit the stress distribution to be measured statically and also to allow dynamic stresses to be measured with the center strain gages at a later time. The A gages were on the putty side of the window and the B gages were directly opposite on the other side of the window. The gage numbers 2, 4, 6, . . . refer to the locations indicated in figure 1. The strain gages were wired into a simple switching network such that each gage in turn could be switched into the same bridge network and the strains read in sequence. The system was temperature compensated by means of conventional techniques.

All the strain gages were read separately; that is, no attempt was made to separate the bending and membrane strains electrically during the static test because one of the purposes of the static test was to proof-test each strain-gage installation. The strain-gage outputs were measured with a conventional static strain indicator. The test procedure for the static test was to take zero readings at zero differential pressure from the strain gages, increase the pressure to the desired test value, hold the pressure constant, take data from the strain gages, and then immediately release the pressure and again take zero readings on all instruments. This technique insured that the zero shift due to temperature was negligible. It was also necessary to check the switch to assure that it was not introducing any varying resistance into one arm of the bridge that would make the readings invalid. No detectable zero shift was observed during the course of any one pressure loading, and the strain gages always returned to the initial zero reading within an accuracy of ± 5 microinches per inch. This check confirmed the validity of the test instrumentation design.

The strain-gage data were checked and corrected, if necessary, for lead-wire resistance effects, distance of foil filament from plate center line, and plate restraint effects. The final strain data are valid to an accuracy of about 5 percent.

RESULTS AND DISCUSSION

Results of Static Measurements

The corrected data from the static tests are tabulated in table I. It should be noted that the difference in the strain readings for gages 6 and 12 was due to the presence of glazier's points at intervals along the edge. These glazier's points changed the edge condition in their immediate vicinity. From this table, the bending and membrane strains are separated and listed in tables II and III, respectively. The maximum total tensile stresses on the low-pressure side of the window (the most highly stressed side) were calculated by using the biaxial stress equations from the strains in table I and are listed in table IV. The bending and

TABLE I.- CORRECTED MEASURED STRAIN AS A FUNCTION OF

UNIFORM STATIC DIFFERENTIAL PRESSURE

[Pressure applied to A gage side of plate;
plus sign denotes tension]

Differential pressure, cm H_2O	Strain, μin./in. for gage -									
	A-2	A-4	A-6	A-8	A-10	A-12	A-14	A-16	A-18	A-20
2	-55	-55	-10	-5	0	-15	-5	-65	-50	+15
4	-75	-65	-20	-5	-5	-40	-10	-130	-85	+15
6	-80	-80	-40	-5	-10	-85	-25	-175	-125	+25
8	-80	-85	-50	-15	-5	-115	-20	-205	-145	+35
10	-75	-75	-55	-15	-10	-130	-15	-225	-170	+45
12	-75	-75	-60	-10	-5	-140	-20	-240	-175	+40
14	-75	-75	-70	-15	-5	-160	-15	-270	-215	+55
Differential pressure, cm H_2O	B-2	B-4	B-6	B-8	B-10	B-12	B-14	B-16	B-18	B-20
2	+55	+55	-10	0	+5	0	+15	+65	+45	-15
4	+95	+95	-50	+20	+25	-40	+50	+95	+75	-25
6	+120	+115	-85	+30	+30	-70	+75	+135	+115	-45
8	+130	+135	-100	+50	+40	-80	+95	+155	+140	-45
10	+145	+150	-125	+65	+55	-115	+120	+175	+170	-55
12	+150	+155	-155	+75	+65	-120	+125	+195	+185	-50
14	+165	+170	-175	+85	+80	-155	+155	+210	+210	-60

TABLE II.- BENDING STRAIN AS FUNCTION OF UNIFORM STATIC DIFFERENTIAL PRESSURE

[Listed results are for B side of plate; A side of plate has same
strain magnitude but opposite sign; plus sign denotes tension]

Differential pressure, cm H_2O	Strain, μin./in. for gage location -									
	2	4	6	8	10	12	14	16	18	20
2	+55	+55	0	+2	+2	+8	+10	+65	+48	-15
4	+85	+80	-15	+13	+15	0	+30	+113	+80	-20
6	+100	+98	-23	+18	+20	+8	+50	+155	+120	-35
8	+105	+110	-25	+33	+23	+18	+58	+180	+142	-40
10	+110	+113	-35	+40	+33	+8	+68	+200	+170	-50
12	+112	+115	-48	+43	+35	+10	+73	+218	+180	-45
14	+120	+123	-53	+50	+43	+3	+85	+240	+212	-58

TABLE III.- MEMBRANE STRAIN AS FUNCTION OF UNIFORM STATIC DIFFERENTIAL PRESSURE

[Strains listed are uniform across the thickness cross section; plus sign denotes tension]

Differential pressure, cm H_2O	Strain, μin./in. for gage location -									
	2	4	6	8	10	12	14	16	18	20
2	0	0	-10	-3	+3	-8	+5	0	-3	0
4	+10	+15	-35	+8	+10	-40	+20	-18	-5	-5
6	+20	+18	-63	+13	+10	-78	+25	-20	-5	-10
8	+25	+25	-75	+18	+18	-98	+38	-25	-3	-5
10	+35	+38	-90	+25	+23	-123	+53	-25	0	-5
12	+38	+40	-107	+33	+30	-130	+53	-23	+5	-5
14	+45	+48	-123	+35	+38	-158	+70	-30	-3	-3

TABLE IV.- DIMENSIONLESS MAXIMUM TOTAL TENSILE STRESS $\sigma a^2/Et^2$ AS FUNCTION OF DIMENSIONLESS UNIFORM STATIC DIFFERENTIAL PRESSURE qa^4/Et^4

FOR B SIDE OF PLATE

[Stress direction is same as that indicated by strain-gage location in figure 1; plus sign denotes tension]

$\frac{qa^4}{Et^4}$	$\sigma a^2/Et^2$ for gage location -									
	2	4	6	8	10	12	14	16	18	20
19.5	+5.95	+5.95	-0.85	+0.15	+0.45	+0.10	+2.60	+5.95	+3.70	-0.45
39.0	+10.25	+10.25	-3.95	+0.71	+1.40	-3.00	+6.30	+9.40	+6.05	-0.70
58.5	+12.95	+12.40	-6.80	+0.85	+1.25	-5.50	+9.30	+13.30	+9.20	-1.65
78.0	+14.05	+14.50	-7.70	+2.35	+1.90	-6.25	+11.45	+15.50	+11.40	-1.15
97.5	+15.60	+16.30	-9.65	+3.15	+2.55	-8.90	+14.05	+17.75	+13.75	-1.40
117.0	+16.20	+16.80	-12.10	+3.40	+3.25	-9.20	+14.90	+19.60	+15.15	-0.60
136.5	+17.75	+18.25	-13.60	+3.95	+3.85	-12.00	+17.75	+21.60	+17.20	-1.05

membrane stresses at the center of the window were calculated, averaged, and plotted in figure 3.

In the upper portion of figure 3 the dimensionless outer-fiber bending stress at the center of the glass panel $\sigma a^2/Et^2$ is plotted as a function of the dimensionless static differential pressure qa^4/Et^4. The experimental stresses are compared with the theoretical predictions obtained by the nonlinear simply supported theory (ref. 7) and also by the linearized simply supported relation (ref. 8), which is valid only for plate center deflections less than the thickness. It can be seen that the measured stresses are somewhat higher than the stresses obtained from nonlinear theory at low static pressures; this difference is perhaps due to uneven support at the edges. At higher values of pressure the measured data agree quite well with the data calculated by the nonlinear simply supported theory. It should be noted that the theoretical curves are calculated for a Poisson's ratio of 0.316 rather than the 0.23 value estimated for the window glass.

The measured membrane stresses at the center of the window are compared with the nonlinear simply supported theory in the lower portion of figure 3, and good agreement is observed.

The total maximum tensile stress at the center of the window is plotted against pressure in figure 4 and compared with data from the linear and nonlinear

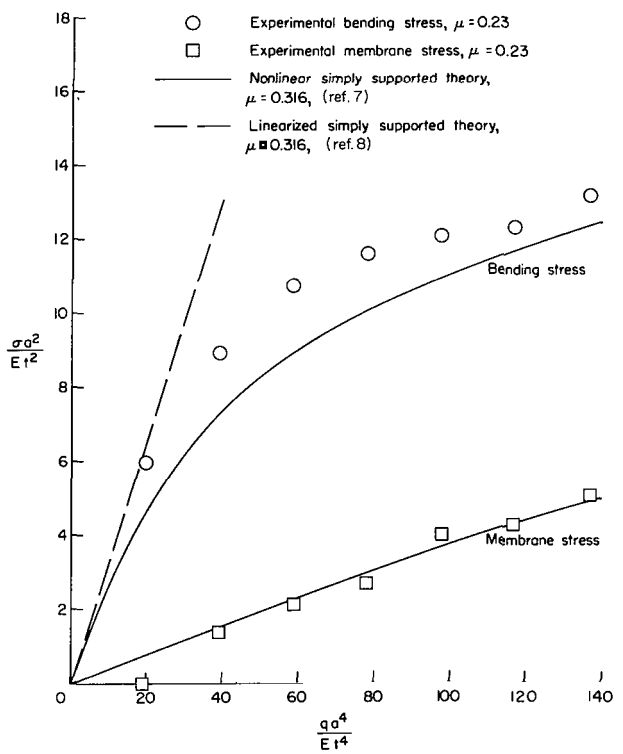

Figure 3.- Outer-fiber bending and membrane stresses at center of window as a function of uniform static pressure.

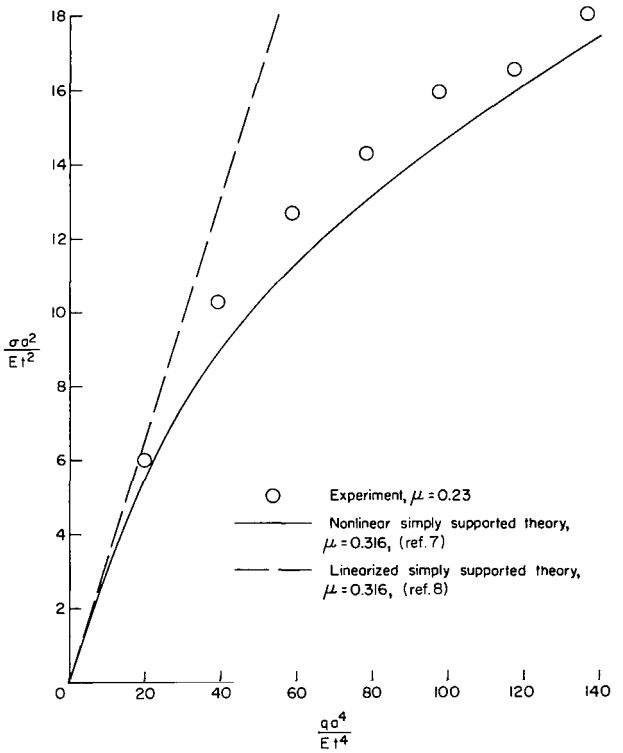

Figure 4.- Total tensile stress at center of window as a function of uniform static pressure.

simply supported theories of references 7 and 8. Again the agreement between the measured data and the data calculated by nonlinear simply supported theory is good. It should be repeated here that it is the maximum tensile stress in the window which causes failure.

The maximum total tensile stress at the center of the panel and at the quarter-diagonal location midway between the center and the edge are compared in figure 5. It can be seen that at low differential pressures, the stresses at the center and quarter-diagonal of the window are very nearly the same. At higher pressures, the quarter-diagonal stress becomes dominant and tends to increase faster than the center stress. Other investigators (refs. 4 and 5) have carefully measured the stress distribution in windows and have concluded that the maximum principal tensile stress in a simply supported square window migrates away from the center of the panel along a diagonal as the load is increased. Furthermore, the location of this stress is some function of the panel deflection, thickness, and span. There is no available theory to support this measured anomaly. Bowles and Sugarman (ref. 5) made a detailed study of the deflection surfaces of square glass plates loaded into the nonlinear range by uniform static pressure. As the load increased into the nonlinear range, a definite flattening of the panel at the center was observed, which was attributed to the membrane stress. Therefore, the region of greatest curvature, and hence maximum bending stress, moved away from the center of the panel with increasing load. In the investigation of reference 5, the panel surface stress distribution was measured; also the plates were loaded to failure. From the measured stresses and the location of the initial failure points, it was concluded that the maximum tensile stress (sum of bending and membrane stress components) for a given load was located at a point on the diagonal and in a direction perpendicular to it.

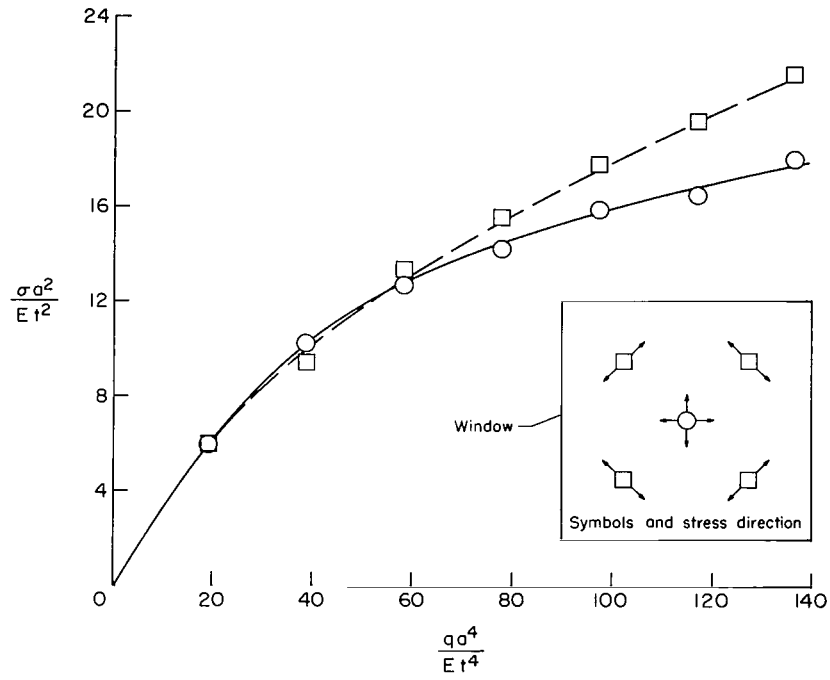

Figure 5.- Total tensile outer fiber stress at center and at quarter-diagonal locations as a function of uniform static pressure.

Discussion of Dynamic Measurements

For the dynamic tests, the window models were exposed to random noise from a large blowdown wind tunnel generating a maximum thrust of 1/2 million pounds for a wide range of sound-pressure levels (ref. 9). For all tests the window was oriented so that a line drawn normal to the plane of the window was also perpendicular to the thrust axis of the jet. The sound was measured with a conventional condenser microphone located near the edge of the window about halfway up and recorded on a portable AM tape recorder. Frequency analyses of this recorded noise were later performed by means of a constant percentage bandwidth analyzer (1/3 octave band). All taped data were corrected for the drop in recorder response below 50 cps.

For purposes of this investigation, the stress at the center of the window was used as the response criterion. The center location is considered the best selection for several reasons. In the fundamental mode of vibration, the center stress provides a reasonable estimate of the maximum stress occurring somewhere along the diagonal. For higher modes of vibration, the center location is preferred as the most suitable location to sample all the odd-numbered modal responses.

For the purpose of reducing the strain-gage instrumentation required, the stress field at the center of the window was assumed to be uniform in all directions. This assumption is strictly true only for the symmetrical mode shapes such as the (1,1), (3,3), (5,5), (7,7), and so on. Some error will be present for the unsymmetrical mode shapes such as the (1,3), (1,5), (3,5), et cetera, but this error was not considered relevant to this study. The four strain gages at the center of the window (fig. 1) were wired into bridges so as to allow bending and membrane strains to be read separately. Provision for measuring bending strains independently of membrane strains was made by wiring the gages on opposite sides of the window into adjacent arms of a bridge. Likewise, measurement of membrane strains independently of bending strains was provided by wiring gages on opposite sides of the window into opposite arms of a bridge (ref. 6). These strain-gage bridges were attached to conventional 3-kilocycle carrier amplifiers and recorded on oscillographs having a flat frequency response from DC to 600 cps. In addition, the output from the bending strain bridge at the center of the panel was recorded on the same tape recorder as the noise record to allow subsequent frequency analysis. For these dynamic tests the window was mounted on the test enclosure illustrated in figure 1.

The fundamental frequency f_o and damping ratio δ of the window were measured by use of a low-amplitude decay damping technique. In free air, f_o was measured as 21 cps and δ as 0.034. Theoretically, f_o was calculated (ref. 10) to be 19 cps for a simply supported edge and 34 cps for a clamped edge. The window was therefore judged to be very nearly simply supported in its frame.

When the window was mounted on the enclosure, the measured fundamental frequency increased to 33 cps because of the stiffness contributed by the air trapped in the enclosure. This frequency agrees well with the calculated value of 31 cps. (See appendix A.) The damping ratio increased to 0.042 when the window was mounted on the enclosure.

Dynamic Test Results

The sound-pressure spectra for the two principal test locations are shown in figure 6. The upper spectrum was measured at a "close" test location 70 feet

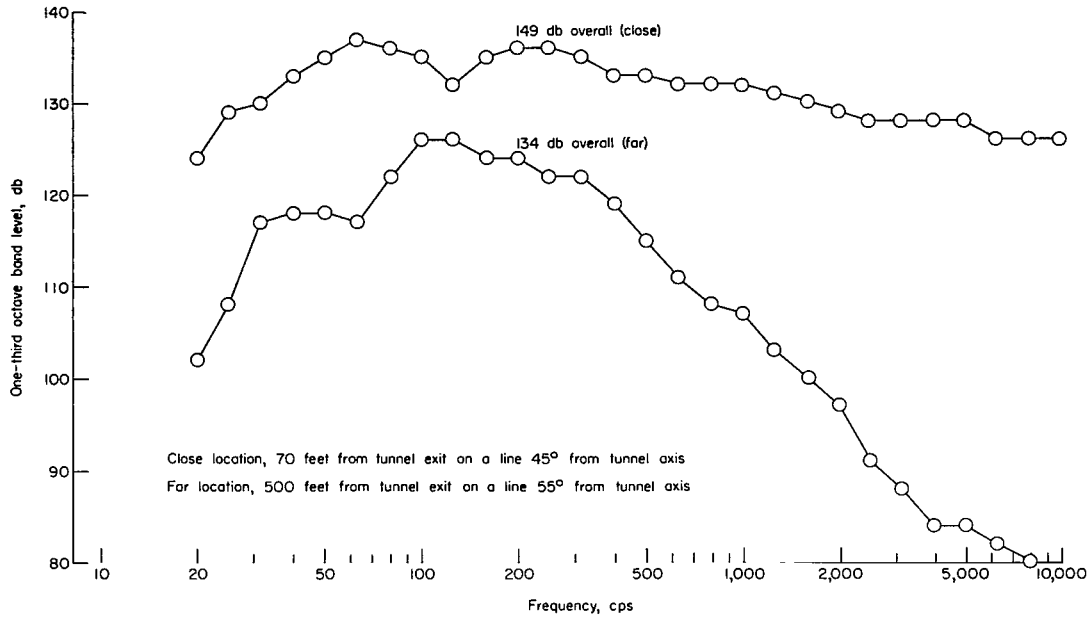

Figure 6.- Sound-pressure spectrum, one-third octave band, for the close and far test locations.

from the tunnel exit and on a line 45° from the tunnel axis. The spectrum shown is very nearly flat. The lower spectrum was measured at a "far" test location 500 feet from the tunnel exit on a line 55° from the tunnel axis.

Bending- and membrane-strain time histories for a relatively low noise level at the far test location are shown in figure 7. The sound-pressure level was 134 db (referenced to 0.0002 dyne/cm^2) overall, and 117 db in a one-third octave band centered at 35 cps, the average fundamental frequency for several test windows. The stresses indicated in the figure were calculated from the strains by using elastic theory as explained in the previous section "Stress Analysis." The bending-strain time history exhibits the appearance of an amplitude modulated sine wave which is the classical response

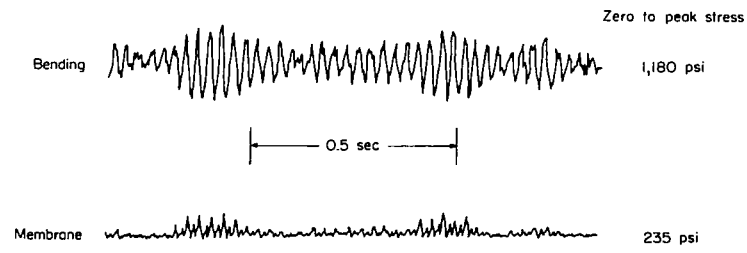

Figure 7.- Bending and membrane stress responses at center of window exposed to an overall random sound-pressure level of 134 db (117 db in a one-third octave band centered at 35 cps) at far location. An upward deflection corresponds to a tensile stress.

of a low damped, single-degree-of-freedom system to a random input. The membrane-strain time history exhibits the appearance of a rectified sine wave, and the magnitudes are relatively small. Hence, the window response at this noise input level can be considered to be very similar to that for a linear system.

At the higher-input sound-pressure levels corresponding to the close test location, the membrane- and bending-strain time histories are markedly different as illustrated in figure 8. The sound-pressure level was 149 db overall and was 132 db in a one-third octave band centered at 35 cps. In this figure the bending stress response no longer exhibits the characteristics of a linear system. There is a definite indication of response in vibration modes of higher order, and this result was observed also by means of high-speed motion pictures. Furthermore, the membrane stresses are of the same order of magnitude as the bending stresses.

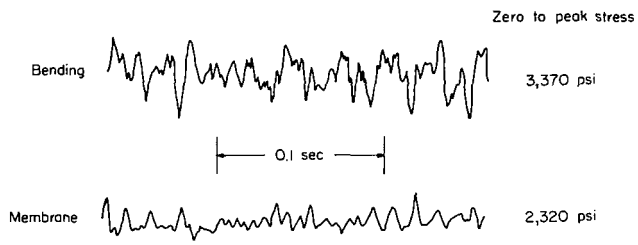

Figure 8.- Bending and membrane stress responses at center of window exposed to an overall random sound-pressure level of 149 db (132 db in a one-third octave band centered at 35 cps) at close location. An upward deflection corresponds to a tensile stress.

For the purpose of evaluating the multimodal responses at the close test location, the bending strain response at the center of one test window was tape recorded, and the frequency was analyzed later by using a continuously variable, narrow-band, constant percentage (8 percent) bandwidth analyzer. The noise level for this test was 136 db overall and 110 db in a one-third octave band centered at 35 cps. This noise spectrum, except for the sound-pressure level, was shaped very nearly the same as the upper spectrum in figure 6. The results for strain are plotted as relative level against frequency in figure 9. The two dominant modes are the fundamental (1,1)

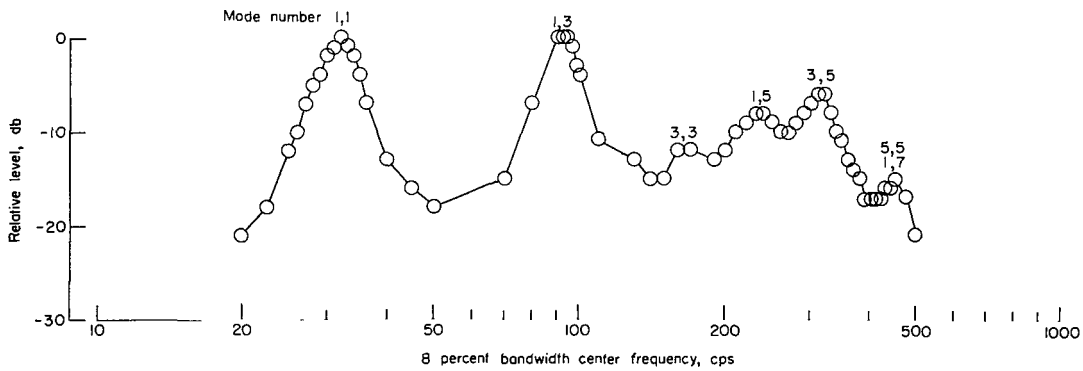

Figure 9.- Level of bending strain (referred to strain at 32 cps) at center of window exposed to an overall random sound-pressure level of 136 db (110 db in a one-third octave band centered at 35 cps).

at 32 cps (appendix A) and the so-called second symmetrical or (1,3) mode at 94 cps. It can be seen in the following table that the measured frequencies for the higher modes of the simply supported plate agree well with theory (ref. 10):

Mode	Measured frequency, cps	Calculated frequency, cps
1,3	94	94
3,3	165	168
1,5	230	244
3,5	315	318
5,5 } 1,7 }	440	468

Note that the odd-numbered modes, which have a net surface displacement, are dominant.

From strain time histories such as those of figures 7 and 8, the peak outer-fiber bending and membrane stresses at the center of the window have been determined and are listed in table V. These stresses are plotted in figure 10 as a

TABLE V.- DYNAMIC TENSILE BENDING AND MEMBRANE STRAINS AND STRESSES AT CENTER OF TEST WINDOWS

Sound-pressure level (one-third octave band at 35 cps), db	Strain, μin./in.			Stress, psi		
	Bending	Membrane	Total	Bending	Membrane	Total
102	24	1	25	310	15	325
104	26	1	27	340	15	355
105	24	1	25	310	15	325
115	62	9	71	805	120	925
117	93	20	113	1,210	260	1,470
117	100	19	119	1,300	245	1,545
118	86	15	101	1,120	195	1,315
118	91	18	109	1,180	235	1,415
118	104	25	129	1,350	325	1,675
120	105	23	128	1,365	300	1,665
124	98	18	116	1,275	235	1,510
124	110	23	133	1,430	300	1,730
126	105	22	127	1,365	285	1,650
126	119	23	142	1,545	300	1,845
134	244	102	346	3,170	1,330	4,500
136	230	102	332	2,990	1,330	4,320
136	184	169	353	2,390	2,200	4,590
136	259	174	433	3,370	2,260	5,630
136	259	178	437	3,370	2,310	5,680

function of the sound-pressure level in a one-third octave band centered at 35 cps. At sound-pressure levels below the 110-db one-third octave band, the bending stresses predominate. At intermediate sound-pressure levels around the

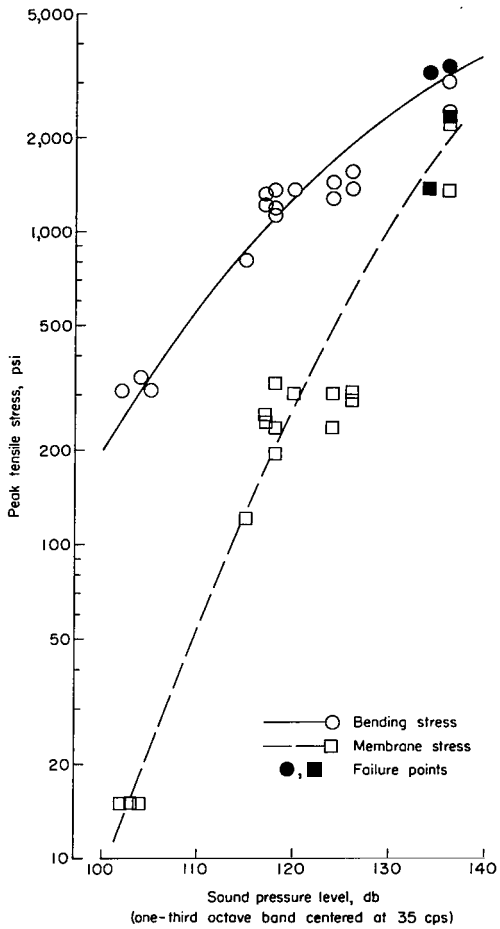

Figure 10.- Peak outer-fiber bending and membrane stress components at center of window exposed to random noise.

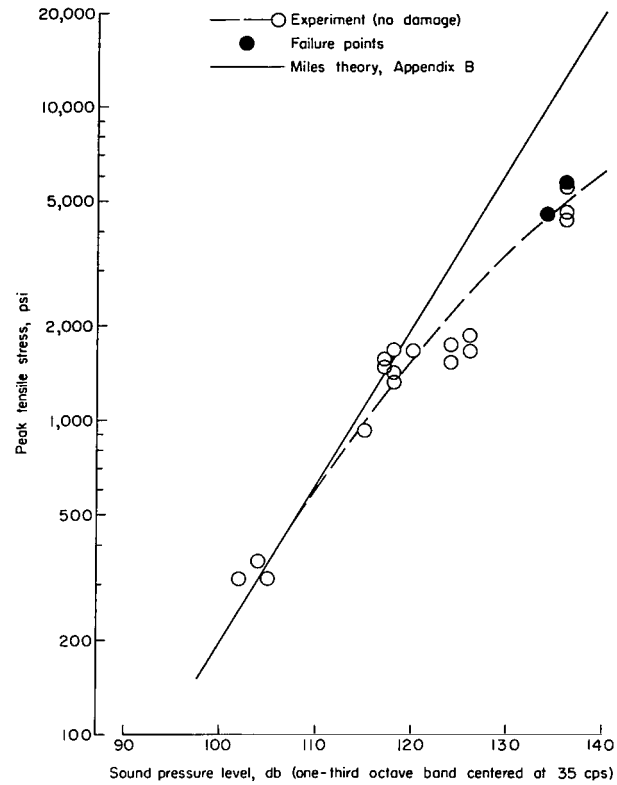

Figure 11.- Total peak outer-fiber tensile stress at center of window due to random noise input.

120-db one-third octave band, the membrane stresses are about 14 db below the bending stresses. At the highest sound-pressure levels of 135 db, the membrane stresses are within 4 db of the bending stresses and are increasing rapidly. Therefore, the window responds in an increasingly nonlinear manner as the noise level increases. The solid circles and squares represent the bending and membrane stresses at failure for two windows. The total tensile stress at the center of the window is the sum of these bending and membrane stresses. This total stress is plotted in figure 11 as a function of the sound-pressure level in a one-third octave band centered at the window fundamental frequency of 35 cps. As in figure 10, the open symbols indicate no apparent damage to the window, whereas the solid symbols are associated with actual failure during tests. The peak stress values increase as the sound-pressure-level values increase, but in a nonlinear manner. Breakage occurred for two models at stress levels of about 4,500 psi and 5,700 psi. These values correspond to one-third octave band sound-pressure levels of 126 db (144 db overall) and 132 db (149 db overall), respectively.

Comparison of Measured Dynamic Response With Theory

Because of obvious interest in the possible prediction of maximum stresses due to random loading in a window, some calculations based on the procedure of Miles in reference 11 have been made (appendix B), and the results are compared with the experimental values in figure 11. It can be seen that good agreement between theory and experiment exists for the low noise input pressures. At higher noise input pressures the measured stresses are lower than the calculated stresses because of the nonlinearity of the stress curves and the multimodal behavior of the model. Thus, the linear theory is applicable only at the lower noise levels for which the window response is approximately linear and occurs primarily in the fundamental mode. At the higher noise levels the linear theory overestimates the window panel stress response because the window is behaving in both a nonlinear and a multimodal manner. It should also be noted that the natural frequency and damping of the plate will change at the larger vibration amplitudes (ref. 12). Furthermore, the simple theory is not strictly correct because the spring stiffness of the enclosure air was neglected.

CONCLUDING REMARKS

The measured stresses at the center of the plate under uniform pressure loading were in good agreement with theory for all values of differential pressure. However, it was observed that the maximum stress in the simply supported plate was located at the center of the plate only for the linear response region. As the response became increasingly nonlinear, the maximum stress location migrated along the diagonals away from the center of the plate, a result that was observed in other recent investigations but is not explained by available theory.

The peak tensile stresses at the center of the plate exposed to random noise were compared with theoretical stresses estimated by the procedure of Miles. Good agreement was observed at low noise levels where the plate response was approximately linear. At higher noise levels the response became increasingly nonlinear in a hard-spring manner and hence the theory overestimated the actual stresses.

Langley Research Center,
National Aeronautics and Space Administration,
Langley Station, Hampton, Va., August 15, 1963.

APPENDIX A

ESTIMATE OF THE FUNDAMENTAL FREQUENCY OF A SIMPLY SUPPORTED PLATE MOUNTED ON AN ENCLOSURE

When the panel is mounted on an enclosure, the apparent fundamental frequency of the window is increased as a result of the stiffness of the air trapped in the enclosure. The spring stiffness of the air in the enclosure is in phase with the physical stiffness of the plate, and hence these stiffnesses add linearly. The following analysis is permissible because the fundamental wavelength of the panel is much greater than the depth of the air column behind the panel.

The fundamental frequency of vibration f is proportional to the square root of the stiffness k:

$$f \propto \sqrt{k}$$

Define

k_1 physical stiffness of panel

k_2 air spring stiffness

f_a frequency of panel due to k_1

f_b frequency of panel due to k_1 and k_2 acting together

The following relations can then be written:

$$f_a \propto \sqrt{k_1}$$

$$f_b \propto \sqrt{k_1 + k_2}$$

Combining these relations yields

$$\frac{f_b}{f_a} = \sqrt{1 + \frac{k_2}{k_1}} \qquad (1)$$

The physical stiffness k_1 of the panel can be described by

$$k_1 = \frac{q_1 A}{w_1}$$

where q_1 is the uniform differential pressure required to deflect the center of the panel an amount w_1.

From the linearized simply supported plate theory (ref. 13), the ratio of pressure to center deflection (for $\mu = 0.3$) is given by

$$k_1 = \frac{q_1 A}{w_1} = \frac{Et^3 A}{0.044a^4} \tag{2}$$

The air spring stiffness can be similarly defined by the uniform pressure change q_2 in the enclosure due to a center deflection w_2 or

$$k_2 = \frac{q_2 A}{w_2} \tag{3}$$

The deflection surface of the fundamental mode can be approximated according to reference 10 as:

$$w = w_2 \cos \frac{\pi x}{a} \cos \frac{\pi y}{a} \tag{4}$$

when the origin of coordinates x and y is located at the center of the plate. The volume of air displaced by this deflected surface is

$$\Delta V = \int_{-a/2}^{a/2} \int_{-a/2}^{a/2} w \, dx \, dy \tag{5}$$

Substituting equation (4) into equation (5) and integrating gives

$$\Delta V = \frac{4a^2}{\pi^2} w_2 \tag{6}$$

To evaluate the corresponding pressure change, consider that this process is very nearly adiabatic in the frequency range of interest. Hence,

$$qV^\gamma = \text{Constant} = q_o V_o^\gamma$$

or

$$\frac{q}{q_o} = \left(\frac{V_o}{V}\right)^{\gamma} \tag{7}$$

where q_o and V_o are the atmospheric pressure and the volume of air trapped in the enclosure, respectively. For a small change in volume and hence in pressure,

$$V = V_o - \Delta V \tag{8}$$

$$q = q_o + \Delta q \tag{9}$$

Introducing equations (8) and (9) into equation (7) yields

$$\frac{q_o + \Delta q}{q_o} = \left(\frac{V_o}{V_o - \Delta V}\right)^{\gamma} = \left(1 - \frac{\Delta V}{V_o}\right)^{-\gamma} \tag{10}$$

Expanding the volume terms in a binomial series and neglecting higher-order terms gives

$$\frac{\Delta q}{q_o} \approx -\gamma \frac{\Delta V}{V_o} \tag{11}$$

Introducing equations (6) and (11) into equation (3) and letting $q_2 = \Delta q$ yields

$$k_2 = \frac{q_2 A}{w_2} \approx \frac{4a^2}{\pi^2} \frac{q_o \gamma A}{V_o} \tag{12}$$

If equations (2) and (12) are substituted into equation (1),

$$\frac{f_b}{f_a} = \sqrt{1 + (0.0179)\frac{q_o \gamma a^6}{V_o E t^3}} \tag{13}$$

Equation (13) can be evaluated, from the known quantities, as

$$f_b = 1.61 f_a$$

The calculated fundamental frequency f_a for the simply supported square plate alone is 19 cps. The calculated fundamental frequency of this same panel, when mounted on the enclosure, therefore, increases to approximately 31 cps.

APPENDIX B

DYNAMIC RESPONSE THEORY

The stress response of a linear, lightly damped, single-degree-of-freedom system to random loads can be estimated by applying Miles' theory (ref. 11) in the following form:

$$\frac{\sigma_{rms}}{S_o} = \frac{p_{rms}(f_o)}{2}\left(\frac{\pi f_o}{\delta}\right)^{1/2}$$

for which the various quantities are

σ_{rms} root-mean-square dynamic stress at center of plate

S_o static stress at center of window per unit static pressure

$p_{rms}(f_o)$ input noise pressure in lb/ft^2 divided by $(bandwidth)^{1/2}$ at panel fundamental frequency

f_o panel fundamental frequency

δ panel damping as fraction of critical damping

For the calculations, S_o was chosen to be 175 psi per lb/sq ft, which is the initial slope of the static bending stress response curve (fig. 3). The panel fundamental frequency f_o was 35 cps, the average for all windows. The damping ratio δ was 0.042, a value measured at low amplitudes of vibration. In order to compare the calculated values with experimental measurements, the ratio of the peak to the rms value of the stress-response time history is assumed to be 3 in all cases. This assumption presumes a Gaussian distribution of stress amplitudes, for which 99.74 percent of all stress amplitudes will be equal to or less than three (3) times the rms stress. This theory is plotted as the straight line in figure 11. Note that the spring stiffness of the enclosure air was not included in this calculation. If it had been included, S_o and, hence, the calculated root-mean-square stress σ_{rms} would have been reduced.

REFERENCES

1. Anon.: Strength of Plate and Laminated Glass. Technical Glass Bulletin, Pittsburgh Plate Glass Co., July 30, 1941.

2. Shand, E. B., et al.: Glass Engineering Handbook. Second ed., McGraw-Hill Book Co., Inc., 1958.

3. Eggwertz, Sigge, and Norr, Artur: Analysis of Thin Square Plates Under Normal Pressure and Provided With Edge Frames of Finite Stiffnesses in the Plane of the Plates. Rep. No. 50, Aeronautical Research Inst. of Sweden, Tekniska Högskolans Rotaprinttryckeri (Stockholm), 1953.

4. Frownfelter, C. R.: Structural Testing of Large Glass Installations. Special Tech. Pub. No. 251, 19, ASTM, 1959.

5. Bowles, R., and Sugarman, B.: The Strength and Deflection Characteristics of Large Rectangular Glass Panels Under Uniform Pressure. Glass Technology, vol. 3, no. 5, Oct. 1962, pp. 156-170.

6. Murray, William M., and Stein, Peter K.: Strain Gage Techniques. Lectures and Laboratory Exercises Presented at M.I.T., 1961.

7. Levy, Samuel: Bending of Rectangular Plates With Large Deflections. NACA Rep. 737, 1942.

8. Timoshenko, S., and Woinowsky-Krieger, S.: Theory of Plates and Shells. Second ed., McGraw-Hill Book Co., Inc., 1959.

9. Mayes, William H., Edge, Philip M., Jr., and O'Brien, James S., Jr.: Near-Field and Far-Field Noise Measurements for a Blowdown-Wind-Tunnel Supersonic Exhaust Jet Having About 475,000 Pounds of Thrust. NASA TN D-517, 1961.

10. Stokey, William F.: Vibration of Systems Having Distributed Mass and Elasticity. Shock and Vibration Handbook, Ch. 7 of Vol. 1 - Basic Theory and Measurements, Cyril M. Harris and Charles E. Crede, eds., McGraw-Hill Book Co., Inc., 1961, pp. 7-1 - 7-41.

11. Miles, John W.: On Structural Fatigue Under Random Loading. Jour. Aero. Sci., vol. 21, no. 11, Nov. 1954, pp. 573-762.

12. Lassiter, Leslie W., and Hess, Robert W.: Calculated and Measured Stresses in Simple Panels Subject to Intense Random Acoustic Loading Including the Near Noise Field of a Turbojet Engine. NACA Rep. 1367, 1958. (Supersedes NACA TN 4076.)

13. Den Hartog, J. P.: Advanced Strength of Materials. McGraw-Hill Book Co., Inc., 1952.

NASA-Langley, 1963 L-3350